Jurnal Kejuruteraan 34(4) 2022: 639-648
https://doi.org/10.17576/jkukm-2022-34(4)-12

Numerical Energy and Exergy Evaluation of a Filament Bulb Controlled Convective Heat Dryer

Stephen A. Ajah[a,b*], Chibuzo V. Ikwuagwu[c] & Benjamin O Ezurike[d]

[a] *Dept. of Mechanical Engineering, Alex Ekwueme University Ndufu-Alike, Ebonyi State*
[b] *Applied Renewable & Sustainable Energy Research Group, Dept. of Mechanical Eng., Univ. of Nigeria, Nsukka, Nigeria*
[c] *African Centre of Excellence for Sustainable Power and Energy Development (ACESPED), University of Nigeria, Nsukka.*
[d] *Dept. of Mechatronic Engineering, Alex Ekwueme University Ndufu-Alike, Ebonyi State*

Corresponding author: stephen.aroh@funai.edu.ng

Received 29 August 2021, Received in revised form 11 October 2021
Accepted 11 November 2021, Available online 30 July 2022

ABSTRACT

The mathematical model for temperature regime thermal analysis evaluation of convective heat dryer has been done. Control volume analysis was adopted in this work while taking note of all the feasible heat transfer mechanisms around the system. Mathematical expressions for the energy, exergy, entropy generation as well as destroyed exergy were derived using the control volume. The consumed energy, exergy, entropy generation and exergy destruction of the dryer were computed. The system temperature gradually increased from its initial room temperature of 270˚C to 720˚C at approximately 2700 secs. The temperature thereafter dropped and stabilized to about 670˚C at 4600 secs while the element dried gradually. The moisture removal curve followed the same trend as that of the temperature with gradual variation from 0.5 to 13.2g/mol. The peak energy from the system is approximately 958J against the useful exergy of 443J which shows that 46.24% of the expended energy was actually useful for the drying purpose and about 10.23% was lost. The energy and exergy efficiencies were also computed and results showed that the efficiencies are functions of temperature just like other influencing parameters which has to be technically controlled. Peak energy efficiency of approximately 54.6% was recorded in the dryer with the peak exergy efficiency of 23.4%. The dryer also yielded a better dried product as compared with the traditional means of drying.

Keywords: Exergy efficiencies; Dryer; Moisture content; Temperature regime evaluation; Exergy destruction

INTRODUCTION

Drying is one of the ancient physical methods of food preservation and other products of organic origin. Its essential purpose is to minimize the moisture content of materials. Predominantly, it is used for preserving food materials like fruits, vegetables, and other products with high degree of moisture (> 80%), as well as others which are considered to be highly perishable (Moses, Alagusundaram, and Tiwari 2014). It involves several approaches, which is a function of both the available means and the predominant atmospheric conditions of a particular geographical location. In some tropical countries, sun drying constitutes an economical and reliable means of preserving agricultural products. According to Hashim et al (Hashim, Daniel, and Rahaman 2014), sun drying involves spreading of wet material under the sun on desirable flat surfaces, hanging wet material on buildings or drying in bundles placed in stalks. Although open-air sun drying remains a cheap processing technique, its limitations include the control of the drying process and parameters, fluctuating weather conditions, big space need, pest invasion, combining with dust and other external particles. In view to minimize high level of post-harvest losses and the challenges of sun drying, other means of dehydration such as solar drying, microwave drying, freeze drying, etc., are used. More than 85% of commercial dryers use convective heat transfer process with either hot air or combustion gases as the working fluid (Moses, Alagusundaram, and Tiwari 2014) which implies that drying is an energy demanding preservative process, hence, it usually accounts for approximately 12-20% of energy used during processing process (Schlünder 2007), (Asiyanbi-Hammed 2016). In this research work, the problem of environmental pollution and carbon monoxide emission witness during drying with firewood, spontaneous burning of the drying sample witnessed with conventional oven is solved while exploiting gradual drying food crops with economic benefit and energy savings. This work aids the evaluation of the temporal behaviour of different samples during drying with respect to their thermo-physical properties which have not been addressed numerically by previous works we consulted.

PHYSICS OF DRYING BIO-PRODUCTS

The main characteristics of this method of preservation is the reduction in the moisture activities in the material thus lowering the product volume, restraining the production of micro-organisms, and minimizing deterioration reactions, thus increasing the product shelf life, efficiency of storage and packaging. Drying is widely used to reduce bulk handling and to guarantee food security during the off-season. The use of dryers can minimize waste of agricultural products and produce better quality of dried product when compared to the local means of drying such as sun or shade drying, this was observed by Doymaz (E. Doymaz 2014) after investigating the outcome of pretreatment using citric acidic mixture with drying temperatures of 40^0C, 50^0C, 60^0C and 70^0C on mushroom slices. It was shown that temperature and pretreatment have reasonable influence on moisture extraction from mushroom. However, drying process sometimes results in the quality reduction of dried products because of high drying temperature as well as the required drying duration. Heat sensitive bio-active constituents for instance, the Overall Phenolic Content (OPC), vitamin C constituent of fruits may be reduced during drying (Edziri et al. 2011). Despite this challenge, dried foods are gaining momentum especially with the growing resistance to the chemical preservation of foods and also for the growing demand for a wider variety of dried foods providing considerable convenience to the consumers. The importance of sustaining the standard measures of the dried agricultural products with considerable retention of bio-active constituents after drying process cannot be overemphasized (Xia 2013). Generally, different drying means will generate varied quality of dried products. For instance, fluidized bed is a short time drying method but it is capable of producing better quality of mushrooms as compared to microwave drying. Vacuum drying is another good substitute because it could help retain the quality of fruits although it requires a longer drying time when compared to microwave drying. Hence drying using microwave produced a degree of undesirable result with short drying duration than the earlier mentioned methods (Chin, S. K., Siew, E. S. and Soon 2015). Higher values of moisture content and temperature for a given product results in a lower value of heat of vaporization. Ekechukwu and Norton (Ekechukwu and Norton 1999) presented the changes of the latent heat of vaporization for some grains with their corresponding moisture content and temperature change during drying.

In the recent years, dryers whether for use in homes or in industries have replaced the traditional method of drying agricultural products because with them drying conditions are controlled for example temperature, moisture content, the drying time, etc. Thus, the final product quality is improved. However, drying should be carried out as economically as possible. A Survey carried out on post-harvest food losses in many Agro-based towns and rural areas in Nigeria showed that approximately 20 – 30% of all grain crops, 30 – 50 % of tuber and root crop as well as a higher percentage of fruits and vegetables are wasted with a great amount observed during storage (Omolola, Jideani, and Kapila 2015). The assumption is that most of these products were lost as a result of inadequate preservation techniques. Considering the prevailing inconsistency in food supply throughout the world, cost- effective and hygienic means of preservation is needful to guarantee food security. Numerous means of food and moist material preservation had been recorded in literature with drying reported to be one of the oldest method (Mustayen, Mekhilef, and Saidur 2014). Drying is a process in which moisture is removed from a wet material by applying suitable energy source mostly in the form of heat. The mechanism of drying is an intricate phenomenon consisting convective transport of heat and mass within the material of interest. Drying is useful in chemical, agricultural, biotechnology, pharmaceutical, pulp and paper, mineral processing, and wood processing industries. The aims of drying are to increase the period of storage, to reduce packaging requirements and to minimize the transportation weight (I. Doymaz 2011). Any designed dryer at a stipulated time is expected to: remove moisture from any product to be dried, produce desired product quality with facilities that satisfy and/or promote environmental sustainability and safety as well as having durable size and being cost effective.

Heat transfer during drying takes place either by one or combination of any two or these three major ways, which are conduction (solids), convection (liquids and gases), and radiation (Kumar, Sarkar, and Sharma 2012), (Sacilik, Keskin, and Elicin 2006). Heat transfer method for a particular application depends on the type of system and the required conditions; heat usually moves from a location of higher thermal potential to a location of lower thermal potential.

To the best of our knowledge and in the literature review conducted, no work has been done whatsoever on convective heat dryer incorporating sensor to monitor/control the drying temperatures. This work is also necessary to preserve the quality of the dried agricultural product with optimal retention of bio-active constituents during drying to minimize product degradation and to retain product quality after drying.

METHODOLOGY

Although, the entire selection process and design of a dryer for a particular purpose is influenced by the motive of obtaining a favourable product quality as well as economical process. But considering several commercial dryers in use most dried products (i.e. vegetables and cereals) are made with convective hot air dryers because it is economical and simple. Even though there are other water or liquid extraction processes in existence such as supercritical removal of liquid from gels, centrifugation, filtration, settling, etc. With these processes, water is extracted by mechanical processes although a significant quantity of liquid is present in the solid material. Four heating bulbs rated 200W each were used in the drying given total power of 800W with total energy loss of approximately 10.9% (Ikwuagwu et al. 2020) from the bulbs. The system design is shown in Figure 1.

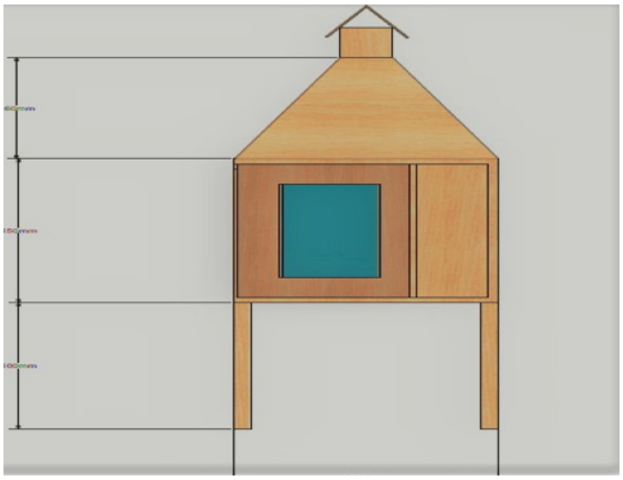

FIGURE 1. The schematic diagram of the convective dryer design

ANALYSIS OF CONVECTIVE HOT AIR DRYER

The above subject matter requires a comprehensive review of heat and mass transfer, thermodynamics and other relative transport theories for analyzing the system.

During the analysis, it was assumed that the drying chamber is perfectly insulated, the heat loss through the vent is negligible, the temperature change between the air at exit and inlet is assumed to be constant and air is assumed to be isotropic.

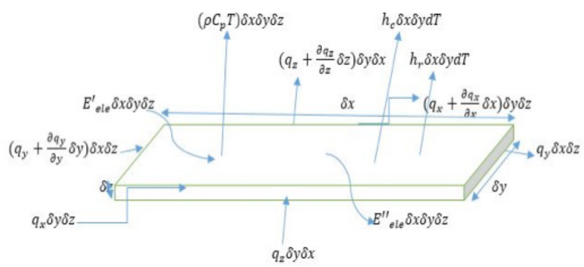

FIGURE 2. Control volume of the drying element

ANALYTICAL ASSUMPTIONS ON THE CONVECTIVE HEAT DRYER

The above subject matter requires a comprehensive review of heat and mass transfer, thermodynamics and other relative transport theories for analyzing the system; the following assumptions were made:

1. The drying chamber is perfectly insulated.
2. The heat loss through the vent is negligible.
3. The temperature change between the air at exit and inlet is assumed to be in transient behaviour.
4. The sliced drying element is assumed to be isotropic.
5. The pressure and density variation in the sliced drying element are infinitesimally small.

Applying the Cartesian coordinate energy equation on the control volume element on the assumption that drying elements are in rectangular shape, we have that:

$$\frac{\partial}{\partial t}(\rho C_p T)\delta x\delta y\delta z = q_x\delta y\delta z - \left(q_x + \frac{\partial q_x}{\partial x}\delta x\right)\delta y\delta z + q_y\delta x\delta z - \left(q_y + \frac{\partial q_y}{\partial y}\delta y\right)\delta x\delta z + q_z\delta y\delta x - \left(q_z + \frac{\partial q_z}{\partial z}\delta z\right)\delta y\delta x + (E'_{el} - E''_{el})\delta x\delta y\delta z - U\delta x\delta y(T_s - T_a) \quad (1)$$

where q_x, q_y and q_z are the heat fluxes across the control surfaces in the x, y and z direction respectively. E'_{el} and E''_{el} and the inflow and outflow electrical energy components. $dT = (T_s - T_a)$ represent the total temperature change between the element surface and the surrounding air. U is the net convective heat transfer coefficient which have been experimentally determined by Ikwuagwu et al (Ikwuagwu et al. 2020). The supposed convective heat loss is reversed back to the system (as it can't leave the system) since the drying chamber is closed and perfectly insulated, it was hence fused with the heat generation term. Simplifying Eqn *1* gives

$$\frac{\partial}{\partial t}(\rho C_p T)\delta x\delta y\delta z = -\frac{\partial q_x}{\partial x}\delta x\delta y\delta z - \frac{\partial q_y}{\partial y}\delta x\delta y\delta z - \frac{\partial q_z}{\partial z}\delta x\delta y\delta z + \left[(E'_{el} - E''_{el}) - \frac{U(T_s - T_a)}{\delta z}\right]\delta x\delta y\delta z$$

Dividing through by $\delta x\delta y\delta z$ gives

$$\frac{\partial(\rho C_p T)}{\partial t} = -\frac{\partial q_x}{\partial x} - \frac{\partial q_y}{\partial y} - \frac{\partial q_z}{\partial z} + \Delta E_{el} \quad (2)$$

But $q_x = -k_x\frac{\partial T}{\partial x}$; $q_y = -k_y\frac{\partial T}{\partial y}$; $q_z = -k_z\frac{\partial T}{\partial z}$

Substituting these into Eqn. 2 gives

$$\rho C_p\frac{\partial T}{\partial t} = k_x\frac{\partial^2 T}{\partial x^2} + k_y\frac{\partial^2 T}{\partial y^2} + k_z\frac{\partial^2 T}{\partial z^2} + \Delta E_{el} \quad (3)$$

Where $\Delta E_{el} = +\left[(E'_{el} - E''_{el}) - \frac{U(T_s - T_a)}{\delta z}\right]$

Dividing 3 by ρC_p gives

$$\frac{\partial T}{\partial t} = \alpha\left[\frac{\partial^2 T}{\partial x^2} + \frac{\partial^2 T}{\partial y^2} + \frac{\partial^2 T}{\partial z^2}\right] + \frac{\Delta E_{el}}{\rho C_p} \quad (4)$$

Since the sliced drying elements are very small, the thermal conductivity remains the same in all directions and at all points within the slice. Hence, we can assume the element to be an isotropic and homogenous medium. So, $k_x = k_y = k_z = k$ and $\frac{k}{\rho C_p} = \alpha$. Therefore, the thermal diffusivity α remain the same everywhere within the sliced element.

Considering the control volume in Figure 2, the temperature variation can be assumed to be in one direction (z-direction), making the problem to be a *1-D* transient problem. Therefore, Eqn. 4 becomes

$$\frac{\partial T}{\partial t} = \alpha\frac{\partial^2 T}{\partial z^2} + \emptyset_{el} \quad (4)$$

From Eqn. 5, $\emptyset_{el}$ is the electrical transient temperature coefficient and $\frac{dT}{dz}$ is the temperature gradient across the element. can be define as

$$\theta = T - T_a$$

From Eqn. (*), $\frac{\partial\theta}{\partial t} = \frac{\partial T}{\partial t}$; $\frac{\partial^2\theta}{\partial z^2} = \frac{\partial^2 T}{\partial z^2}$; $\frac{d\theta}{dz} = \frac{dT}{dz}$;. Therefore, Eqn. 5 becomes

$$\frac{\partial\theta}{\partial t} = \alpha\frac{\partial^2\theta}{\partial z^2} + \emptyset_{el} - \vartheta_c\frac{d\theta}{dz} \tag{6}$$

Eqn. 5 can be solved numerically by discretization to get the temporal temperature variation of the sliced element and the moisture drop of the element during the drying process. Considering the control volume discretization in Figure 3, the sliced element of thickness *Hm* is subdivided into *n* times of Δz each.

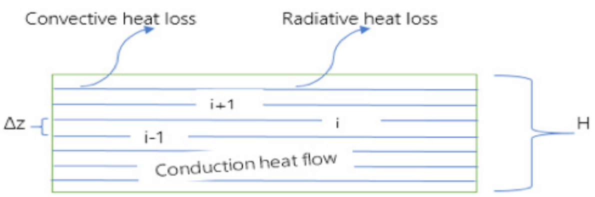

FIGURE 3. Discretized elemental control volume

Taking the temporal notation to be *k* and the space notation to be *i*, the central reference node of the CV is taking as *i*, moving upward from the central node is given as *i+1*, *i+2*, ……… *n*, moving downward from the central node is given as *i-1*, *i-2*, ……. *1*. Eqn. 5 can be discretized as:

$$\frac{T_i^{k+1} - T_i^k}{\Delta t} = \alpha\left[\frac{T_{i+1}^k - 2T_i^k + T_{i-1}^k}{(\Delta z)^2}\right] + \emptyset_{el}^k \tag{7}$$

Simplifying Eqn. 7 gives

$$T_i^{k+1} - T_i^k = \frac{\alpha\Delta t}{(\Delta z)^2}\left(T_{i+1}^k - 2T_i^k + T_{i-1}^k\right) + \emptyset_{el}^k\Delta t \tag{8}$$

$$T_i^{k+1} = T_i^k(1 - 2Fo) + Fo\left(T_{i-1}^k + T_{i+1}^k\right) + \emptyset_{el}^k\Delta t \tag{9}$$

Eqn. 9 gives the temporal temperature variation within the intermediate nodes of the elemental volume due to conduction heat flow, where *Fo* is the mesh Fourier number given as $\frac{\alpha\Delta t}{(\Delta z)^2}$.

INITIAL AND BOUNDARY CONDITIONS

Initially, the temperature and the corresponding moisture concentration of the elemental piece is respectively given as T_0 and C_{i0}. Considering the lower boundary of the elemental slice, the slice is resting on a perforated pan which is thermally serving as an insulator when compared to the heat transfer rate on the surface of the slice. The radiative and convective heat loss on the bottom surface can be assumed to be zero since it is infinitesimally small when compared to that on the upper surface. Hence,

$$\left.\frac{\partial T}{\partial z}\right\}_{z=0} = 0 = \rho C_p A\frac{\Delta z}{2}\frac{\partial T}{\partial t} - kA\frac{\partial T}{\partial z} - \Delta E_{el}A\frac{\Delta z}{2} \qquad bci$$

$$\left.\frac{\partial T}{\partial z}\right\}_{z=H} = \rho C_p A\frac{\Delta z}{2}\frac{\partial T}{\partial t} - kA\frac{\partial T}{\partial z} - \Delta E_{el}A\frac{\Delta z}{2} - h_c A dT_n - h_r A dT_n \qquad bcii$$

$$\rho C_p A\frac{\Delta z}{2}\left(\frac{T_1^{k+1} - T_2^k}{\Delta t}\right) = kA\left(\frac{T_1^k - T_2^k}{\Delta z}\right) + \Delta E_{el}A\frac{\Delta z}{2} \tag{10}$$

Where $A = \delta x\delta y$.

$$\frac{T_1^{k+1} - T_2^k}{\Delta t} = 2\alpha\left(\frac{T_1^k - T_2^k}{(\Delta z)^2}\right) + \frac{\Delta E_{el}}{\rho C_p} \tag{11}$$

Simplifying Eqn. 11 gives

$$T_1^{k+1} - T_2^k = \frac{2\alpha\Delta t}{(\Delta z)^2}(T_1^k - T_2^k) + \emptyset_{el}^k\Delta t \tag{12}$$

$$T_1^{k+1} = T_2^k + 2Fo(T_1^k - T_2^k) + \emptyset_{el}^k\Delta t \tag{13}$$

$$T_1^{k+1} = T_2^k(1 - 2Fo) + 2FoT_1^k + \emptyset_{el}^k\Delta t \tag{14}$$

Eqn. 14 gives the temporal temperature variation within node 1 of the elemental volume due to conduction heat flow. Considering the upper surface of the elemental slice, convective and radiative heat losses are taking place even though it is within the drying chamber but the drying chamber is thermally interacting with the ambient. Therefore, the energy balance on the node can be given as

$$\rho C_p A\frac{\Delta z}{2}\left(\frac{T_n^{k+1} - T_{n-1}^k}{\Delta t}\right) = kA\left(\frac{T_n^k - T_{n-1}^k}{\Delta z}\right) + \Delta E_{el}A\frac{\Delta z}{2} + h_c A(T_\infty^k - T_n^k) + h_r A(T_s^k - T_n^k) \tag{15}$$

Where h_c and h_r are the convection and radiation heat transfer respectively, T_∞^k is the temporal ambient temperature and T_s^k is the temporal drying chamber surface temperature. Simplifying Eqn. 15 further,

$$T_n^{k+1} - T_{n-1}^k = \frac{2k\Delta t}{\rho C_p(\Delta z)^2}(T_n^k - T_{n-1}^k) + \frac{\Delta E_{el}\Delta t}{\rho C_p} + \frac{2h_c\Delta t}{\rho C_p\Delta z}(T_\infty^k - T_n^k) + \frac{2h_r\Delta t}{\rho C_p\Delta z}(T_s^k - T_n^k) \tag{16}$$

$$T_n^{k+1} = T_{n-1}^k + 2Fo(T_n^k - T_{n-1}^k) + \emptyset_{el}^k\Delta t + 2FoBi_c(T_\infty^k - T_n^k) + 2FoBi_r(T_s^k - T_n^k) \tag{17}$$

Where Bi_r and Bi_c are the radiative and convective Biot number associated with the respective radiation and convection heat transfer on the surface node.
Eqn. 17 can further be simplified as:

$$T_n^{k+1} = T_{n-1}^k(1 - 2Fo) + T_n^k[2Fo(1 - Bi_c - Bi_r)] + \emptyset_{el}^k\Delta t + 2FoBi_cT_\infty^k + 2FoBi_rT_s^k \tag{18}$$

Eqn. 18 gives the temporal temperature variation on the last node (node *n*) of the elemental volume due to conduction heat flow. Eqn. 9, Eqn. 14 and Eqn. 18 can be combined to get the net temporal temperature variation within the elemental slice given as T^{k+1}. Bi_c and Bi_r in Eqn. 18 are given as $\frac{h_c\Delta t}{k}$ and $\frac{h_r\Delta t}{k}$ respectively.

Since the drying chamber is perfectly insulated, the increase in internal energy per unit mass of the yam is equivalent to the thermal energy requirement for the evaporation of unit mass of moisture content within the drying element. Hence,

$$h_c A_s(T^{k+1} - T_a) = \dot{m}h_{fg_w} = h_D A_s(C_i^{k+1} - C_a)h_{fg_w} \tag{19}$$

h_D is the mass transfer coefficient, A_s is the heat/mass transfer surface area, $\dot{m}$ is the moisture evaporation rate, h_{fgw} is the latent heat of vaporization of the moisture and C_i^{k+1} is the temporal surface moisture concentration and C_a is the drying chamber moisture concentration. But if there is high temperature in the drying chamber during the heating process such that the temporal moisture concentration of the element behaves like an ideal gas within the chamber and it is strictly a function of the temporal temperature variation and the pressure assumed to be constant, the moisture concentration can be related to the temperature change within the dryer. Hence,

$$C_i^{k+1} = \frac{M_i p_i}{R_m T^{k+1}} \tag{20}$$

But in real case where assumption leading to Eqn. 20 is not applicable, the heat transfer can be related to the mass transfer energy required. From Eqn. 19, the moisture evaporation rate is evaluated as

$$\dot{m} = \frac{h_c A_s (T^{k+1} - T_a)}{h_{fgw}} \tag{21}$$

The temporal moisture concentration difference can as well be evaluated from Eqn. 19 as

$$C_i^{k+1} - C_a = \frac{h_c (T^{k+1} - T_a)}{h_D h_{fgw}} \tag{22}$$

From Eqn. 19,

$$\frac{h_c}{h_D} = \rho C_p \left(\frac{Sc}{Pr}\right)^{2/3} = \rho C_p (Le)^{2/3} \tag{23}$$

Where *Le* is Lewis number given by $\left(\frac{\propto}{D}\right)$. Substituting Eqn. 23 into Eqn. 22 yields

$$C_i^{k+1} = C_a + \rho C_p (Le)^{2/3} \frac{(T^{k+1} - T_a)}{h_{fgw}} \tag{24}$$

If is assumed to be zero (infinitesimally low moisture concentration),

$$C_i^{k+1} = \rho C_p (Le)^{2/3} \frac{(T^{k+1} - T_a)}{h_{fgw}} \tag{25}$$

At the surface of the element, both heat, mass and momentum transfer are simultaneously taking place within the chamber in a turbulence manner. This requires correlation using Chilton-Colburn j-factor which implies that

$$j_H = j_D = \frac{C_f}{2} \tag{26}$$

Eqn. 26 can also be referred to as heat, mass and momentum transfer analogy, while C_f is the skin friction factor, for the case of flow over a flat plate (like this case), it is given as

$$C_f = \frac{1.288}{Re_L^{1/2}} \text{ (for laminar case)} \tag{27}$$

$$C_f = \frac{0.074}{Re_L^{0.2}} \text{ (for turbulent case)} \tag{28}$$

$$j_H = \frac{h_c}{\rho v C_{p,a}} Pr^{2/3};\ j_D = \frac{h_D}{v} Sc^{2/3}$$

For flow over a flat plate, the heat transfer coefficient is given as a correlation:

$$h_c = 0.037 Re_L^{-1/5} \rho v C_{p,a} Pr^{-2/3} \tag{29}$$

$$h_r = \varepsilon\sigma(T_s + T_n)(T_s^2 + T_n^2) \tag{30}$$

Similarly, the mass diffusion coefficient h_D is given by

$$h_D = 0.037\, v\, Re_L^{-1/5} Sc^{-2/3} \tag{31}$$

Where ρ is the air density, v is the air velocity, $C_{p,a}$ is the specific heat capacity of air. The Reynold number, Re_L, Prandtl number *Pr* and Schmidt number *Sc* are respectively given as:

$$Re_L = \frac{\rho v L}{\mu};\ \mathrm{Pr} = \frac{C_{p,a}\,\mu}{k};\ Sc = \frac{\upsilon}{D}$$

Where μ is the air absolute viscosity, υ is the kinematic viscosity of air, L is the heat flow surface length.

For the thermal properties of the drying element (Dioscorea dumetorum specifically), Oluwamukomi and Akinsola (Oluwamukomi and Akinsola 2015) worked on the thermal and physicochemical properties of some starchy foods. Oke et al (Oke, Ogunlakin, and Philip 2009) through their studies modelled the thermophysical properties of yam like thermal conductivity (k), density (ρ) specific heat capacity (C_p) and thermal diffusivity (α) as purely temperature dependent variables.

$$k = 0.164 + 0.001T + 7.676 * 10^{-7} T^3 \tag{32}$$

$$\rho = 1100.49 + 4.107T + 0.004T^2 - 0.004T^3 \tag{33}$$

$$C_p = 2750.89 + 2.693T - 2.925T^2 - 0.069T^3 \tag{34}$$

$$\alpha = \frac{k}{\rho C_p} \tag{35}$$

The energy consumed by the dryer in drying any particular amount of element can be calculated as

$$E_{con} = m_y C_p (T^{k+1} - T_{ini}) \tag{36}$$

Where T_{ini} is the initial temperature of the element, T^{k+1} is the final temperature of the element, C_p is the specific heat capacity of the element while m_y is the mass of the element dried.

The anergy generation by the system can as well be calculated as

$$\emptyset_{gen} = T_a \Delta S \tag{37}$$

Where ΔS is the change in entropy of the element and can be evaluated on assumption of negligible pressure change as

$$\Delta S = m_y \left[C_p In\left(\frac{T^{k+1}}{T_{ini}}\right) + RIn\left(\frac{P^{k+1}}{P_{ini}}\right) \right] \tag{38}$$

The pressure term in Eqn. 38 $\left(\frac{P^{k+1}}{P_{ini}}\right)$ is neglected as infinitesimal pressure change is observed. From Eqn. 36, 37 and 38, the useful exergy of the system can be evaluated as

$$\Xi_{con} = m_y C_p \left[(T^{k+1} - T_{ini}) - T_a In\left(\frac{T^{k+1}}{T_{ini}}\right) - T_a R / C_p In\left(\frac{P^{k+1}}{P_{ini}}\right) \right] \tag{39}$$

The input energy to the system is the electrical energy used in the heating/drying process which is given by

$$E_{in} = IV * t_{tot} \tag{40}$$

Where is the total drying time (sec). The input exergy of the system can as well be given as

$$\Xi_{in} = E_{in}\left(1 - \frac{T_{ini}}{T^{k+1}}\right) \tag{41}$$

If Eqn. 36 is divided by Eqn. 40, the energy efficiency of the system can be gotten and the exergy efficiency of the system can be evaluated when Eqn. 39 is divided by Eqn. 41.

$$\eta_I = \frac{E_{con}}{E_{in}} \tag{42}$$

$$\eta_{II} = \frac{\Xi_{con}}{\Xi_{in}} \tag{43}$$

RESULTS AND DISCUSSION

The modelled equations were solved with Scilab using numerical approach for data computation. From Oke et al (Oke, Ogunlakin, and Philip 2009), the thermal properties of the tested species as a function of the element temperature were also computed using Eqn. 32 to 35. Where Eqn. 35 can be computed from Eqn. 32, 33 and 34. The temporal thermophysical properties were used in solving Eqn. 9, 14, 18, 21, 25, 36, 37, 38, 39 and 41 for the computation of the temporal temperature, surface moisture evaporation rate, moisture content, consumed energy, anergy generation/exergy destruction, entropy change and useful exergy of the system respectively. The energy and exergy efficiencies of the system were as well computed from Eqn. 42 and 43.

TEMPERATURE AND CONCENTRATION PROFILE

Figure 4 shows the temporal temperature profile and moisture concentration removal against the drying time of the element. It can be observed from the graph that the temperature gradually increased from the normal room temperature of 27˚C at zero secs time to 72˚C at approximately 2700 secs (45 mins) as the peak temperature. The temperature thereafter dropped to 67˚C due to thermal and microscopic particulate agitation of the drying element. During this period, the chemical and intermolecular bonds of the drying element and their contained water get loose and break away which always demand much thermal energy and then drops the thermal profile of the system. The thermal profile therefore stabilized at 67˚C at 4600 secs (approximately 1 hour, 17 mins) as the agitation decreases and the element was gradually dried due to this temperature control measure because there was no further increase in temperature of the element. In a similar manner from Figure 4, the moisture removal curve followed the same trend as the temperature profile and remain nearly constant at the same time temperature remain constant (i.e. from 0.5 to 13.2 g/mol). Since the drying chamber is well insulated, the space can easily be saturated with the evaporating moisture at constant temperature

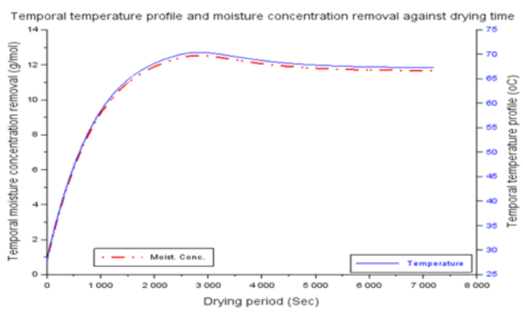

FIGURE 4. Temperature and concentration profile

The moisture concentration removal amount and the surface evaporation rate were also plotted against the drying time to compare them. With the temperature control (moisture concentration removal as a function of temporal temperature), similar trend is applicable in surface evaporation rate as in the case of moisture concentration removal. The surface evaporation rate gradually increased from nearly 0.001 g/s to 0.0142 g/s. The rate of the surface evaporation is slightly more than the moisture concentration removal just after 900 secs (15 mins) even though they maintain the same rate from the onset of the drying till that period. Meanwhile, the difference between the two parameters became higher at nearly the peak temperature time and maintain the amplitude after the temperature remain constant.

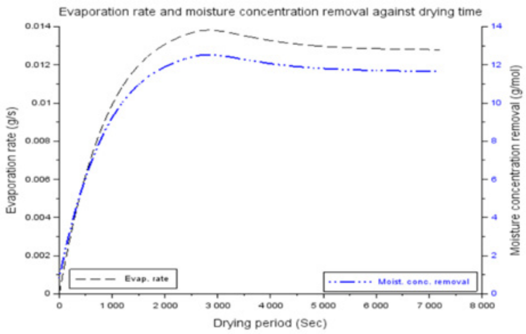

FIGURE 5. Evaporation rate and concentration profile

CONSUMED ENERGY AND EXERGY

The energy and exergy consumed within the system in addition to the convective heat lost in the system were plotted against the drying time in Fig 6 just like the other parameters. From the graph, the convection heat loss in the system is relatively low due to the drying chamber heat loss preventive measures. The useful exergy of the system can be seen to be more than the convective heat loss though less than the energy consumed in the system. This justified the reason for the insulation of the dryer and the second law definition of exergy of a system. This will result to efficient drying system though the entropy generation minimization will further make the system more efficient. The peak energy computed from the system is approximately 958 J against the useful exergy which is about 443 J. The peak of both parameters occurred nearly at the same time with that of the temperature. This implies that temperature control all other drying parameters in the system since the air flow within the drying chamber is very low. Comparing the energy consumed and the useful exergy of the system at the peak level from Figure 6, it can be observed that about 46.24% of the expended energy was actually useful for the drying purpose and about 10.23% were lost due to convective heat loss. This also implies that much energy was lost through exergy loss accompanying heat and energy generation (i.e. exergy destruction).

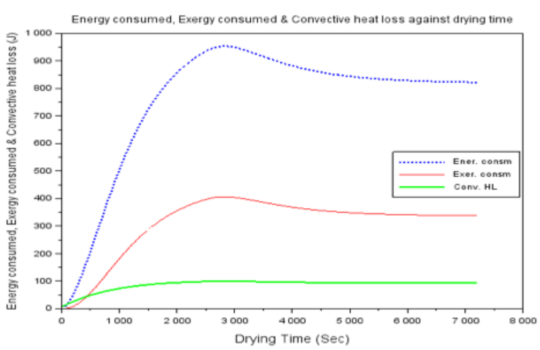

FIGURE 6. Energy and exergy consumed with the convective heat loss during the drying

ENTROPY GENERATION RATE IN THE SYSTEM

Figure 7 shows the plot of the entropy generation and the consumed exergy of the system. It can be observed that higher entropy is generated than the exergy utilized in the system due to the irreversibility in the dryer. As the drying time increases, the difference between the exergy and entropy generation rate increases even after the point of constant temperature. This justified the fact that even at constant temperature (in this case of temperature-controlled dryer), irreversibility like element bond breaking results to further entropy generation.

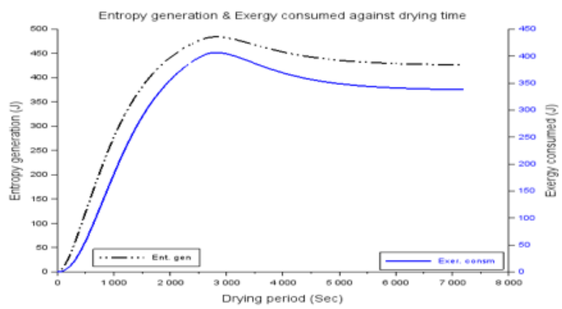

FIGURE 7. Entropy generation and exergy consumed during the drying

EFFICIENCIES OF THE SYSTEM

The consumed system energy and exergy efficiencies were plotted against the drying time of the element in Figure 8. Both efficiencies were observed to follow the same trend as the expended energy and exergy. Peak energy efficiency of approximately 54.6% was recorded in the dryer with the peak exergy efficiency of 23.4%. The peak of both efficiencies occurred nearly at the same time.

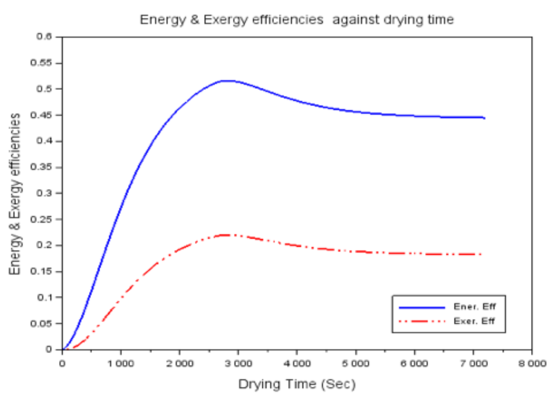

FIGURE 8. Energy and exergy efficiencies of the system

VALIDATION OF THE MODELS

The validation of the models was done by matching of the results gotten from the model with those of the experimental results of the same dryer after the design and construction by Ikwuagwu et al (Ikwuagwu et al. 2020). Figure 9 shows the prototype after different stages of the dryer design and fabrication at Mechanical Engineering workshop, University of Nigeria, Nsukka.

FIGURE 9. Final dryer prototype

Figure 10 also shows the experimental testing of the dryer. Different sliced pieces of Trifoliate yam were dried in the fabricated dryer at different temperatures to test the dryer functionality and efficiency.

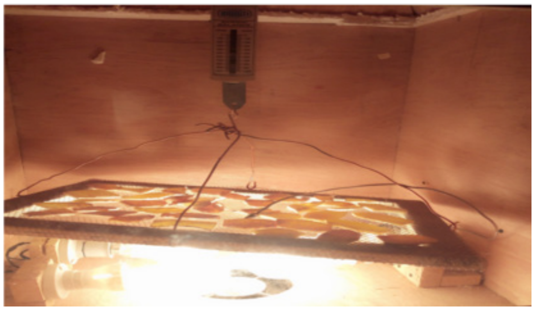

FIGURE 10. Drying of Trifoliate Yam

The yams were cut to dimensions of 50 mm by 30 mm by 5 mm as used in the model of this particular study. The sliced yams were put on top of perforated rectangular pan and placed over four 200W filament bulbs as can be seen in Figure 10.

Figure 11 shows the plot of the experimental data of the evaporation rate against time at 70^{0}C. Comparing the plot of Figure 11 with that of Figure 5 and Figure 4, it can be observed that the data from the model conformed to that of the experimental result. The experimental results also show that 70^{0}C temperature is the best mild drying temperature of the yam due to their thermo-physical properties which is also in line with the model result in Figure 4.

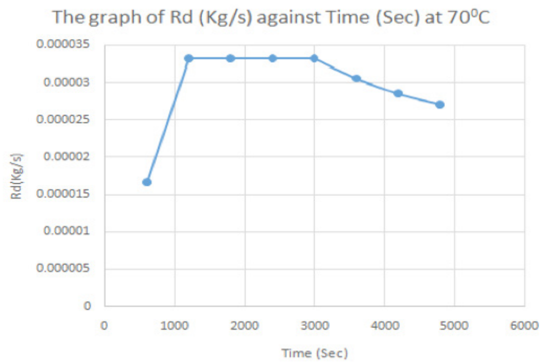

FIGURE 11. Graph of evaporation rate against time (sec) at 70$^\circ C$

CONCLUSIONS

The mathematical model for the thermal analysis for temperature regime evaluation of convective heat dryer has been done. The consumed energy, exergy, entropy generation, exergy destruction and efficiencies of the dryer had been computed as well. The performance of the dryer has been examined by drying Dioscorea dumetorum with gradual temperature variation and the results obtained show that:

1. The drying time and other thermal parametric influence of the dryer is a function of the dryer's operating temperature.
2. The dryer's efficiency was also computed and results showed that the efficiencies are functions of temperature. It also yielded better products as compared with the traditional means of drying.
3. The required power for the dryer is as small as 800 W (four 200 W filament bulbs), hence a portable generator of 900 W or 1 kW can be used to power the system to account for energy transmission losses.
4. The numerically modelled dryer was not location-specific as it can be applied anywhere with the consideration of the location ambient temperature in the model, hence any agricultural product can be dried in it provided the drying temperature is specified, and this implies making relevant modifications if needed.

From the results, it can be observed that the optimal performance with optimum efficiency of the dryer can be achieved around temperature of between 65˚C to 72˚C if technically maintained through gradual heating. The moisture content of yam is usually between 56 − 78%, hence a high moisture content of 75% was used for the analysis. By implication, an agricultural product of high moisture content can be dried in the dryer provided it is set on a desired temperature as the controlling parameter.

ACKNOWLEDGMENT

The authors of this research paper wish to express their profound gratitude to the workers in Department of Mechanical Engineering workshop, University of Nigeria, Nsukka, Enugu State, Nigeria for the facilities used to carry out the experiments.

DECLARATION OF COMPETING INTEREST

None

REFERENCES

Asiyanbi-Hammed, Tawakalit Tope. 2016. North Dakota State University.

Chin, S. K., Siew, E. S. and Soon, W. L. 2015. Drying characteristics and quality evaluation of kiwi slices under hot air natural convective drying method. *International Food Research Journal* 22 (6): 2188–95.

Doymaz, E. 2014. Drying kinetics and rehydration characteristics of convective hot-air dried white button mushroom slices. *Journal of Chemistry* 2014: 1–9. https://doi.org/http://dx.doi.org/10.1155/2014/453175.

Doymaz, I˙brahim. 2011. Thin-layer drying characteristics of sweet potato slices and mathematical modelling. *Heat Mass Transfer* 47 (2011): 277–85. https://doi.org/10.1007/s00231-010-0722-3.

Edziri, H L, M A Smach, S Ammar, M A Mahjoub, Z Mighri, M Aouni, and M Mastouri. 2011. Antioxidant, antibacterial, and antiviral effects of lactuca sativa extracts. *Industrial Crops & Products* 34 (1): 1182–85. https://doi.org/10.1016/j.indcrop.2011.04.003.

Ekechukwu, O. V. and B. Norton. 1999. Review of solar-energy drying systems II : An overview of solar drying technology. *Energy Conversion & Management* 40: 615–55.

Hashim, Norhashila, Onwude Daniel, and Ezdalina Rahaman. 2014. A preliminary study : Kinetic model of drying process of pumpkins (cucurbita moschata) in a convective hot air dryer. *Italian Oral Surgery* 2: 345–52. https://doi.org/10.1016/j.aaspro.2014.11.048.

Ikwuagwu, Chibuzo V, Stephen A Ajah, Nwokenkwo Uchenna, Nwigwe Uzoma, Udochukwu J. Anuta, Ogba Chinedu, and Onu Emmanuel. 2020. Development of an Arduino-Controlled Convective Heat Dryer. In *UNN International Conference: Technological Innovation for Holistic Sustainable Development (TECHISD2020)*, 180–95.

Kumar, Navneet, B C Sarkar, and H K Sharma. 2012. Mathematical modelling of thin layer hot air drying of carrot pomace. *J Food Sci Technol (January–February* 49 (February): 33–41. https://doi.org/10.1007/s13197-011-0266-7.

Moses, J. A., K. Alagusundaram, and B. K. Tiwari. 2014. Novel drying techniques for the food industry. *Food Eng Rev* 6: 43–55. https://doi.org/10.1007/s12393-014-9078-7.

Mustayen, A. G. M. B., S. Mekhilef, and R. Saidur. 2014. Performance study of different solar dryers : A review. *Renewable and Sustainable Energy Reviews* 34: 463–70. https://doi.org/10.1016/j.rser.2014.03.020.

Oke, Moruf, Grace Oluwatoyin Ogunlakin, and Sobukola Olajide Philip. 2009. Some thermo-physical properties of yam cuts of two geometries. *African Journal of Biotechnology* 8(7): 1300–1304.

Oluwamukomi, M. O., and O. O. Akinsola. 2015. Thermal and physicochemical properties of some starchy foods : Yam (dioscorea rotundata), cocoyam (xanthosoma sagittifolium) and plantain (musa paradisiaca). *Food Science and Technology* 3(1): 9–17. https://doi.org/10.13189/fst.2015.030102.

Omolola, Adewale O, Afam I O Jideani, and Patrick F Kapila. 2015. "Quality Properties of Fruits as Affected by Drying Operation." *Food Science and Nutrition*, no. February: 37–41. https://doi.org/10.1080/10408398.2013.859563.

Sacilik, Kamil, Rahmi Keskin, and Ahmet Konuralp Elicin. 2006. Mathematical modelling of solar tunnel drying of thin layer organic tomato. *Journal of Food Engineering* 73: 231–38. https://doi.org/10.1016/j.jfoodeng.2005.01.025.

Schlünder, E. 2007. Drying of porous material during the constant and the falling rate period : A critical review of Existing Hypotheses. *Drying Technology: An International Journal* 22 (June 2013): 37–41. https://doi.org/10.1081/DRT-120038738.

Xia, K A I. 2013. Dynamics of convective hot air drying of filiform lagenaria siceraria. *Chemical Industry & Chemical Engineering Quarterly* 19(4): 485–93. https://doi.org/10.2298/CICEQ120313082Z.

Nomenclature		
q_z	heat fluxes across the control surfaces in the x direction	W/m^2
E'_{el}	Inflow rate volumetric electrical energy	W/m^3
E''_{el}	Outflow rate volumetric electrical energy	W/m^3
T_s	Surface temperature of the drying sample	˚C
T_a	Surface temperature of the drying sample	˚C
α	Thermal diffusivity	m^2/s
C_p	Specific heat capacity	J/kgK
ρ	density	kg/m^3
k	Thermal conductivity	W/mK
Δt	Change in time	sec
T	Temperature of the drying sample	˚C
A	Area	m^2
h_c	Convection heat transfer coefficient	W/m^{2}K
h_r	Radiation heat transfer coefficient	W/m^{2}K
Bi_c	Convection heat transfer Biot number	
Bi_r	Convection heat transfer Biot number	
Fo	Fourier number	
Le	Lewis number	
h_D	Convective mass transfer coefficient	m/s
μ	Absolute viscocity	Kg/s.m
υ	Kinematic viscocity	m^2/s
v	Air velocity	m/s
σ	Stefan-Boltzmann constant	
Re	Rhenold number	

Nomenclature contn'd		
Pr	Prandtl number	
Sc	Schmidt number	
h_{fgw}	latent heat of vaporization of the moisture	J/kg
$\dot{m}$	moisture evaporation rate	Kg/s
$\emptyset_{el}$	internal transient heat generation coefficient	T/s
θ	Temperature difference	˚C
C_f	skin friction factor	
C_a	Initial moisture concentration	Kg/s
j_D	Chilton-Colburn j-factor for mass transfer	

Nomenclature contn'd		
j_H	Chilton-Colburn j-factor for heat transfer	
L	heat transfer surface length	m
Subscripts and superscripts		
k	temporal notation	
i	space notation	
n	space notation for the last node	
s	surface	
a	air	
c,r	convective, radiative	